This is an open access article published under an ACS AuthorChoice License, which permits copying and redistribution of the article or any adaptations for non-commercial purposes.

Macromolecules

Article

pubs.acs.org/Macromolecules

Expanding the Dimensionality of Polymers Populated with Organic Robust Radicals toward Flow Cell Application: Synthesis of TEMPO-Crowded Bottlebrush Polymers Using Anionic Polymerization and ROMP

Takashi Sukegawa, Issei Masuko, Kenichi Oyaizu,* and Hiroyuki Nishide*

Department of Applied Chemistry, Waseda University, Tokyo 169-8555, Japan

Supporting Information

ABSTRACT: Poly(norbornene)-*g*-poly(4-methacryloyloxy-2,2,6,6-tetramethylpiperidin-1-oxyl) (PNB-*g*-PTMA) was prepared by a grafting-through approach based on anionic polymerization of 4-methacryloyloxy-2,2,6,6-tetramethylpiperidin-1-oxyl using a norbornene-substituted diphenylhexyllithium to yield a norbornene-functionalized macromonomer (NB-PTMA) and subsequent ring-opening metathesis polymerization of NB-PTMA using a Grubbs third-generation catalyst, which avoided critical side reactions involving the nitroxide radical of TEMPO moiety. The anionic polymerization resulted in high yields (>94%), narrow polydispersity indices (<1.20), and radical concentrations (0.95 radicals per monomer unit). The ROMP also resulted in high yields (>98%) and high radical concentrations (0.95 radicals per monomer unit), by virtue of the functional group tolerance of these reactions. Single molecular dimension of PNB-*g*-PTMA was measured by dynamic light scattering and by atomic force microscopy (AFM), which precisely reflected the bottlebrush structure to reveal the presence of the TEMPO group crowded at the periphery of the molecule. The lengths of PNB-*g*-PTMA along the macromolecular side chains and the polynorbornene main chain were both approximately equal to the theoretical lengths estimated by the degree of polymerization for each chain. The number-average diameter of PNB-*g*-PTMA in THF increased with initial NB-PTMA ratio to the Grubbs catalyst. Photo-cross-linked thin layer electrodes of PNB-*g*-PTMA demonstrated the reversible redox reaction at 0.80 V vs Ag/AgCl corresponding to the TEMPO/TEMPO$^+$ couple and quantitative charging/discharging processes even at 120 C rate (i.e., full charging in 30 s). As a novel application of redox-active polymers, PNB-*g*-PTMA exhibited 95% efficiency of the theoretical charge capacity in a flow cell system, based on the unique properties of bottlebrush polymers such as the defined molecular dimension and relatively low solution viscosity in comparison with corresponding linear polymers.

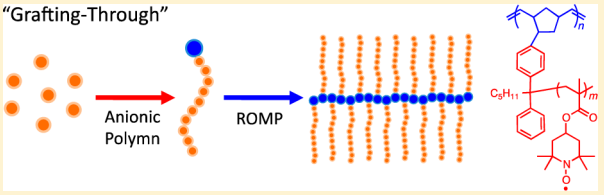

INTRODUCTION

Electrochemical energy storage requires a couple of dissimilar electroactive materials on current collectors separated by an electroinactive electrolyte layer.[1] Recent progress in organic electrode-active materials[2,3] is based on the finding of redox-active molecules such as viologens,[4] quinones,[5−9] *N*-cyclic polyketones,[10−12] conjugated carbonyl compounds,[13−15] and fused heteroaromatic compounds[16−19] that stay on current collectors without dissolution into the electrolyte layer during charging−discharging cycles. However, inherent dissolubility of these molecules has made resistive gel electrolytes and/or ion-exchange membranes indispensable to suppress self-discharge caused by a redox shuttle effect. Organic batteries that permit the use of less resistive porous separators, like those of Li-ion batteries, have been developed by using particular polymers which survive on the current collector and yet maintain their activity as a result of enhanced exchange reaction between highly populated redox-active sites bound to aliphatic main chains.[20−22] In fact, molecular design of organic electrodes from the viewpoints of the mass- and electron-transfer processes is essential to improve the performance of the organic battery.[1] We anticipated that polymers should also help to replace the porous separator for ion-exchange membranes that are currently employed to fractionate the electroactive fluids in flow batteries, especially when the electroactive polymers possess discrete molecular sizes in a mesoscale.[23] Here we report the synthesis of a redox-active bottlebrush polymer characterized by an expanded dimensionality from those of linear analogues and the excellent charge storage capability accomplished by the polymer solution, with potential application to the flow battery applications.[24]

We have been focusing on robust organic radical-containing polymers with superior charge-transport and -storage properties based on the reversible electrode reactions of the radical molecules such as 2,2,6,6-tetramethylpiperidin-1-oxyl (TEMPO) and their fast electron exchange reactions via the densely populated radical sites[25−35] and have proposed them as the electroactive materials for electronic devices such as organic

Received: August 7, 2014
Revised: November 17, 2014
Published: December 16, 2014

 © 2014 American Chemical Society dx.doi.org/10.1021/ma501632t | *Macromolecules* 2014, 47, 8611−8617

batteries,[36−47] dye-sensitized solar cells,[48−53] nonvolatile memories,[54,55] electrochromic displays,[56−58] and electrochemical diodes.[59] A radical polymer forms an amorphous layer on a current collector and moderately swells in electrolyte solutions, allowing the electrolyte ions and the solvent molecules to swim smoothly throughout the polymer layer concurrently with the redox reaction of the radical molecules. Electrochemical properties of the radical polymers in organic radical-based batteries are typically embodied in advantages such as the high charging/discharging rate (120 C i.e., full charging/discharging in 30 s), the high charge capacity (>140 mAh g^{-1}), and the long cycle stability (over 1000 cycles).[60−62] Linear homopolymer, with which slight cross-linking was sometimes utilized to enhance the cycle stability of radical polymer electrodes, has been adopted as the basic structure of the radical polymers to demonstrate the excellent electrochemical properties. On the other hand, architectures of other electroactive polymers have been intensely investigated in the range of nano- to microscale. For example, monomer sequence, stereoregularity, and phase separation of different components in a block copolymer have been examined because of their tremendous impacts on device performances.[63−65] We have revealed notable effects of polymer structures on the charge transport involving the radical molecules; network-type radical polymers increase the effective distance of the charge transport through the polymer layers compared to linear radical polymers, and well-ordered radical-containing block copolymers modulate charge transport in response to morphology.[66,67] The mechanisms of these charge transport are under investigation, but the examples indicate that polymer architecture is a promising viewpoint to design radical polymers.

Bottlebrush polymers containing densely and regularly grafted polymeric side chains on a macromolecular backbone have persistent shapes, which are sustained by steric repulsion between the polymeric side chains and are controlled by the lengths of both the side chain and the backbone. The single molecular dimension of bottlebrush polymers and the viscosity of their solutions are small compared to corresponding linear polymers with the same molecular weight due to the multi-branched structures.[68,69] The spatially tunable structures of bottlebrush polymers provide unique applications such as cylindrical templates, nanotubes, photonic materials, and photoresist materials, in which bottlebrush polymers are utilized in the forms of unimolecular or assembled materials in nanoscales.[70−75]

Redox-active radical molecules have potential to incorporate electrochemical properties to bottlebrush polymers leading to redox-active nano-objects as shape-persistent organic electroactive materials. The TEMPO-crowded bottlebrush polymer is indeed an attractive target of synthetic challenge. Recently, well-defined bottlebrush polymers were mostly synthesized by "grafting-to", "grafting-from", and "grafting-through" strategies using combinations of living/controlled polymerizations and click chemistry.[76−81] Controlled radical polymerizations such as atom transfer radical polymerization, reversible addition−fragmentation chain transfer polymerization, and nitroxide-mediated radical polymerization are often used for the synthesis of well-defined bottlebrush polymers.[82−87] However, as represented by nitroxide-mediated radical polymerization, potential reactivity of the nitroxide radical of the TEMPO moiety with propagating carbon radicals inhibits radical polymerization of the radical-bearing monomers,[88] which have led us to examine the radical polymerization of secondary amine-containing radical precursors and following oxidation of the resultant polymers as a basic approach to synthesize the radical polymers.[89] The oxidation process sometimes inherently triggers side reactions such as unnecessary cross-linking of the polymer and fails oxidation of every radical precursor to result in limited radical concentration. Therefore, well-controlled polymerizations of the radical monomers, which overcome these problems, are required for the synthesis of the bottlebrush polymers typically with multiple-step reactions.

We have recently developed living polymerizations of nitroxide radical monomers using anionic polymerization and ring-opening metathesis polymerization (ROMP),[90−93] which demonstrate adequate tolerance for nitroxide radical moieties. Thus, we selected a "grafting-through" strategy using anionic polymerization and ROMP to synthesize the TEMPO-crowded bottlebrush polymers. Norbornene-terminated polyTMA (NB-PTMA) was synthesized by anionic polymerization using norbornene-substituted diphenylhexyllithium as an initiator. PTMA-grafted poly(norbornene) (PNB-*g*-PTMA) was subsequently synthesized via ROMP of NB-PTMA macromonomer. The architectures of PNB-*g*-PTMA were characterized by dynamic light scattering and atomic force microscopy measurements. The redox potential corresponding to TEMPO and quantitative charging/discharging capacity of PNB-*g*-PTMA represents the capability of PNB-*g*-PTMA as a redox-active nanomaterial. We also preliminarily report superior charging/discharging performance of PNB-*g*-PTMA solution in a flow cell based on the solution properties of the bottlebrush polymer.

RESULTS AND DISCUSSION

Synthesis of Norbornene-Substituted Diphenylhexyllithium (NB-DPHLi) for Anionic Polymerization. NB-DPHLi, which contains the diphenylhexyllithium (DPHLi) portion as an initiator for anionic polymerization of 4-methacryloyloxy-2,2,6,6-tetramethylpiperidin-1-oxyl (TMA) to yield a norbornene-terminated polyTMA (NB-PTMA) macromonomer and the norbornene portion as a monomer for ring-opening metathesis polymerization (ROMP) of the NB-PTMA macromonomer to yield a radical bottlebrush polymer via a grafting-through approach, was synthesized (Scheme 1). The compact structure of NB-DPHLi, in which the norbornene directly links to DPHLi without any spacer, is rationally designed in terms of cell capacity because extra segments irrelevant to redox reactions reduce the theoretical capacity of the radical bottlebrush polymer. Furthermore, the C−C bond directly connecting norbornene with DPHLi was also selected to avoid undesired transformations of NB-DPHLi which were observed in reactions between butyllithium and diphenylethylene (DPE) containing leaving groups such as alkoxymethyl on the *para*-position.[94] The structurally compact concept in NB-DPHLi is analogous to radical-substituted norbornene monomers in our previous report,[87] and therefore, we adopted a formation of C−C bond using a Pd catalyst to connect norbornene and DPE as the synthetic approach for the key compound norbornene-substituted DPE (NB-DPE). NB-DPE was simply synthesized by the three-step sequence consisting of palladium-catalyzed coupling reaction, Grignard reaction, and dehydration reaction. After purification by column chromatography, NB-DPE was obtained as a pure white solid confirmed by NMR spectroscopy and elemental analysis. The mixture solution of NB-DPE and *n*-butyllithium yielded a deep red color solution owing to the reaction between the DPE

dx.doi.org/10.1021/ma501632t | *Macromolecules* 2014, 47, 8611−8617

Scheme 1. Synthesis of Radical Bottlebrush Polymer PNB-*g*-PTMA

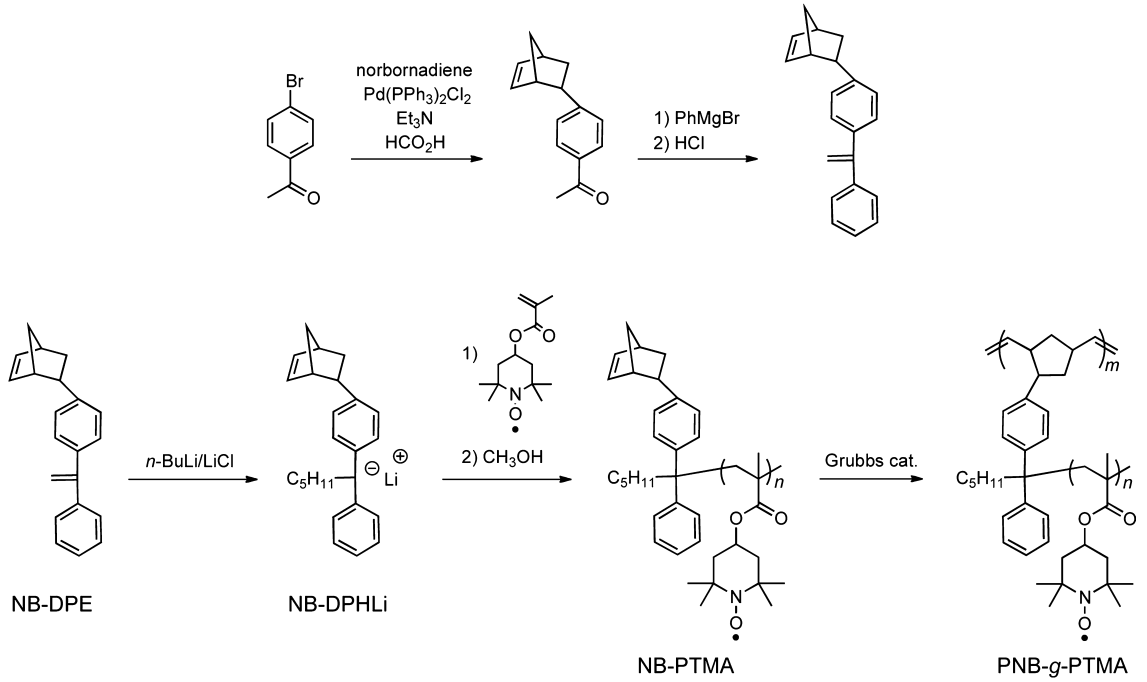

portion and *n*-butyllithium to form NB-DPHLi. The alkene in the norbornene portion of NB-DPE was stable against the nucleophilic attack of *n*-butyllithium through the preparation of NB-DPHLi according to a ^{1}H NMR spectrum of the crude product after reaction between NB-DPE and *n*-butyllithium (Figure S1). The ^{1}H signal of the alkene in the norbornene portion at 6.19−6.28 ppm existed with an integrated area value equal to that before the reaction while the ^{1}H signal of the alkene in the diphenylethylene portion at 5.45 ppm decreased.

Synthesis of Norbornene-Terminated PTMA Macromonomer (NB-PTMA). NB-PTMA macrmonomers were synthesized via the anionic polymerization of TMA monomer using NB-DPHLi initiator. The results of the anionic polymerization are summarized in Table S1. *n*-BuLi was added to 1.2 mol equiv of NB-DPE in THF at −61 °C, and then the solution was stirred to be red color corresponding to NB-DPHLi. The solution immediately turned from red to colorless after the addition of small amount of the TMA monomer solution due to the initiation reaction between DPHLi and methacrylate moiety of the TMA monomer and then turned pale orange corresponding to TEMPO during the addition of the remaining TMA monomer solution. The resultant polymers were obtained with low PDIs (<1.2), quantitative yields (>94%), and high radical concentrations (2.38×10^{21} unpaired electrons/g, i.e., 0.95 radicals per monomer unit) estimated by superconducting quantum interface device (SQUID), which confirmed that the anionic polymerization was effective to prepare the TEMPO-containing macromonomers. Furthermore, a MALDI-TOF MS spectrum of NB-PTMA showing multipeaks corresponding to the molecular weights, which were equal to the sum of the NB-DPH unit and the TMA monomer sequence at a regular intervals of the monomer molecular weight, indicated that each macromonomer was end functionalized with norbornene, which acted as a monomer unit for ROMP (Figure S2).

Synthesis of Polynorbornene-*g*-PTMA (PNB-*g*-PTMA). ROMP of NB-PTMA was carried out in toluene at room temperature using both Grubbs second- and third-generation catalysts (G2 and G3, respectively), which have high tolerance toward nitroxide radicals. The polymerization results are summarized in Table 1. ROMP of NB-PTMA ($M_n = 6.1 \times 10^3$)

Table 1. Ring-Opening Metathesis Polymerization of NB-PTMA Macromonomer[a]

entry	M_n NB-PTMA (10^3 g/mol)	$[NB\text{-}PTMA]_0/[C]_0$	conv[b] (%)	M_n[b] (10^4 g/mol)	PDI[b]
1	3.4	25	99	3.2	1.17
2	3.4	50	99	5.8	1.18
3	3.4	100	98	8.4	1.33
4	6.1	50	98	23	2.73
5	6.1	50	98	9.0	1.29
6	6.1	100	99	12	1.36
7	6.1	200	99	15	1.62

[a]Conditions: Grubbs third-generation catalyst (entries 1−3 and 5−7), Grubbs second-generation catalyst (entry 4), 40 mM for norbornene unit in toluene, at RT, 12 h. [b]Determined by GPC using polystyrene standard in 0.1 M LiCl/DMF.

using G2 at the molar ratio of $[NB\text{-}PTMA]_0/[G2]_0 = 50$ resulted in 98% conversion estimated by GPC, while the PDI of the obtained PNB-*g*-PTMA bottlebrush polymer was relatively high (PDI = 2.73) rather ascribed to the reactivity of G2, which was characterized by relatively slow rate of the initiation reaction compared to that of the propagation reaction. ROMP using G3 under the identical condition, except for the catalyst, however, resulted in 98% conversion and relatively narrow PDI (= 1.29) compared to ROMP using G2. PNB-*g*-PTMA polymers were successfully obtained via ROMP even at the higher macromonomer ratio ($[NB\text{-}PTMA]_0/[G3]_0 = 100$ and 200) with high conversion (>98%) and narrow PDIs (<1.62). GPC curves for each bottlebrush polymer shifted to higher molecular weight along with the [NB-PTMA]/[G3] ratio (Figure 1). PNB-*g*-PTMA polymers consisted of NB-PTMA

dx.doi.org/10.1021/ma501632t | *Macromolecules* 2014, 47, 8611−8617

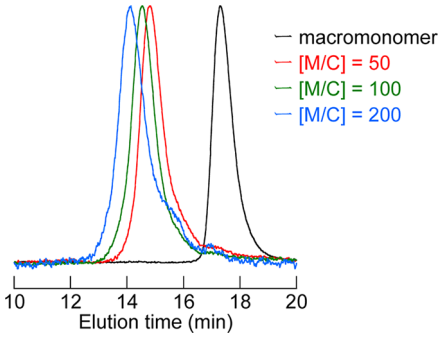

Figure 1. GPC traces of the macromonomer NB-PTMA (M_n = 6100, black), crude brush polymers PNB-*g*-PTMA obtained at [M/C] = 50 (red), 100 (green), and 200 (blue).

macromonomers with other chain lengths were also prepared in high conversion (>98%) and narrow PDIs (<1.33). The increments of the differences between the experimental and the theoretical values for molecular weight and the PDI values of PNB-*g*-PTMA along with [NB-PTMA]/[G3] ratio were attributed to the size differences at the same molecular weights between PNB-*g*-PTMA bottlebrush polymers and linear polystyrenes for GPC calibration standards. A unimodal electron spin resonance (ESR) spectrum was obtained for a PNB-*g*-PTMA/CH_2Cl_2 solution at the *g*-value = 2.0064 due to the spin exchange interaction between the unpaired electrons of the neighboring nitroxide radicals, in contrast to the three-line spectrum for TEMPO with the distinct hyperfine structure. A high radical concentration of PNB-*g*-PTMA (2.38×10^{21} unpaired electrons/g, i.e., 0.95 radicals per monomer unit) estimated by SQUID, which was equal to the radical concentration of the NB-PTMA macromonomer, indicated that ROMP of NB-PTMA had no side reaction involving the nitroxide radical of the TEMPO moiety. These results confirmed that ROMP of NB-PTMA using G3 was a well-controlled polymerization as well as ROMP of other radical-substituted norbornenes and other norbornene-terminated macromonomers.

Structure Analysis of PNB-*g*-PTMA. Sizes of PNB-*g*-PTMA bottlebrush polymers were measured by dynamic light scattering (DLS). The DLS measurements were conducted at 25 °C for NB-PTMA macromonomer/THF solutions of both NB-$PTMA_{3400}$ ($M_n = 3.4 \times 10^3$) and NB-$PTMA_{6100}$ ($M_n = 6.1 \times 10^3$) and for the correspondent PNB-*g*-PTMA/THF solutions, which were prepared after removal of the extra toluene as the solvent and ethyl vinyl ether as a termination reagent for the polymerizations by evaporation without further purification (Figure 2). The number-average diameter of

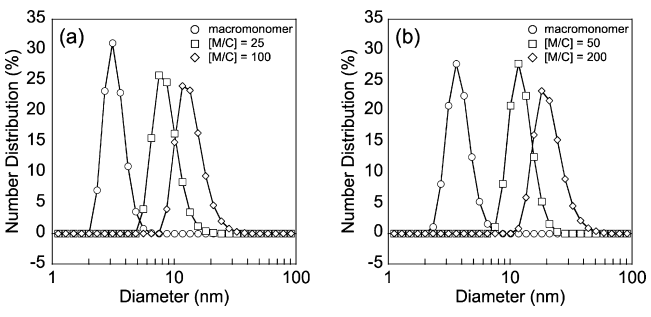

Figure 2. Hydrodynamic diameter plots obtained using DLS for (a) NB-PTMA (M_n = 3400) and PNB-*g*-PTMA ([M/C] = 25 and 100), (b) NB-PTMA (M_n = 6100), and PNB-*g*-PTMA ([M/C] = 50 and 200).

PNB-*g*-$PTMA_{3400}$ increased along with the increment of molecular weight from 9 ± 2 nm ($M_n = 3.2 \times 10^4$, entry 1 in Table 1) to 14 ± 4 nm ($M_n = 8.4 \times 10^4$, entry 3 in Table 1), which were larger than 3 ± 1 nm for NB-$PTMA_{3400}$. PNB-*g*-$PTMA_{6100}$ also exhibited the same tendency on the diameter from 14 ± 4 nm ($M_n = 9.0 \times 10^4$, entry 5 in Table 1) to 21 ± 6 nm ($M_n = 1.5 \times 10^5$, entry 7 in Table 1), which were larger than 4 ± 1 nm for NB-$PTMA_{6100}$. Moreover, the histograms of DLS measurements for each PNB-*g*-PTMA had no index for the NB-PTMA macromonomers. These results further confirmed that the ROMP of NB-PTMA using G3 achieved the high conversion even at $[NB\text{-}PTMA]_0/[C]_0 = 200$ without noticeable interference such as the side reaction related to the nitroxide radical of the TEMPO moiety. The structure of PNB-*g*-PTMA was visualized by atomic force microscopy (AFM). A sample was prepared by drop-casting of a PNB-*g*-$PTMA_{5800}$ ($M_n = 1.0 \times 10^5$, $[NB\text{-}PTMA]_0/[C]_0 = 50$)/THF dilute solution on a highly ordered pyrolytic graphite (HOPG) substrate and drying under ambient conditions. The AFM phase image of PNB-*g*-$PTMA_{5800}$ showed an interwoven pattern consisted of single molecules isolated on the HOPG substrate (Figure 3a). The flat surface of the sample with less than 1 nm in height roughness (Figure 3b,c) and the orientation of the bottlebrush polymers along three main directions, which was affected by the hexagonal lattice of HOPG surface as well as other branched polymers, proved that bottlebrush polymers formed a monolayer on the HOPG substrate. The size of the rodlike individual radical polymers was 5−6 nm in width and 30−40 nm in length, along PTMA side chains and polynorbornene backbone, respectively. Considering 2.5 Å of all-trans vinylic chain length and 6.2 Å of norbornene length per monomeric unit of each macromonomer and bottlebrush polymer,[81,95] the theoretical size of a fully stretched PNB-*g*-$PTMA_{5800}$ was 5.8 nm in the width and 31 nm in the length, which well accorded with the observed size of PNB-*g*-$PTMA_{5800}$.

Electrochemical Properties of PNB-*g*-PTMA. Cyclic voltammograms of PNB-*g*-PTMA displayed reversible waves at $E_{1/2}$ = 0.80 V vs Ag/AgCl with the negligible peak to peak separation ΔE_p (= $E_{pa} - E_{pc}$) (Figure S5a), which was ascribed to the redox reaction between the nitroxide radical and the oxoammonium cation of the populated TEMPO pendants regardless of the molecular weight of the bottlebrush polymers. The cyclic voltammogram indicated that PNB-*g*-PTMA most likely adsorbed on the platinum working electrode through the redox reactions. Thin layer electrodes of PNB-*g*-$PTMA_{9000}$ ($M_n = 4.6 \times 10^4$, thickness ϕ = 380 nm) on ITO electrodes, which were insoluble but swollen in common electrolyte solutions, were prepared by photo-cross-linking utilizing a cyclization of the olefin moiety of the polynorbornene backbone with the nitrene originated from a bisazide derivative. A half-cell fabricated with the thin layer electrode demonstrated a reversible redox wave at $E_{1/2}$ = 0.80 V vs Ag/AgCl, a characteristic potential to PNB-*g*-PTMA (Figure 4a). The chronopotentiogram of the cell exhibited a plateau potential at 0.82 V, which agreed with the $E_{1/2}$ of the electrode, the quantitative capacity 103 mAh/g which was 96% of the theoretical capacity (107 mAh/g), and long cycle life maintained over 90% of the initial capacity after 100 cycles (Figure 4b). Furthermore, the thin layer electrode demonstrated a remarkably high current density with rapid charging/discharging at 120 C rate (i.e., 30 s per each charging and discharging), maintaining over 80% capacity of the full charging. The diffusion coefficient for the propagating charge ($D = 1.6 \times 10^{-10}$ cm^2 s^{-1}) determined from

dx.doi.org/10.1021/ma501632t | *Macromolecules* 2014, 47, 8611−8617

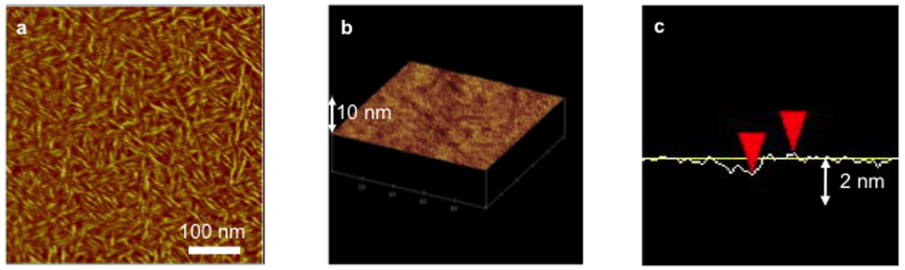

Figure 3. AFM (a) phase and (b) height images of the PNB-*g*-PTMA$_{5800}$ bottlebrush polymer (M_n = 1.0 × 10^5, [NB-PTMA]$_0$/[C]$_0$ = 50) layer. (c) A cross-sectional profile of the layer.

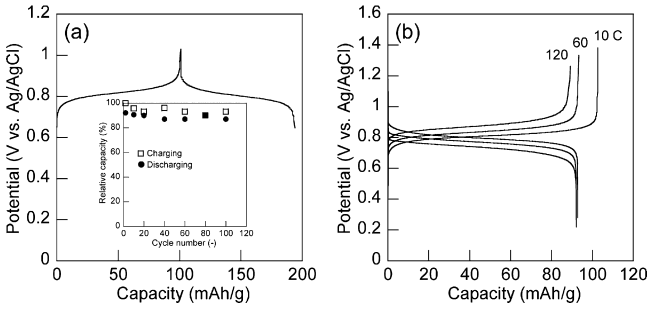

Figure 4. Charging/discharging curves of the PNB-*g*-PTMA (M_n = 4.9 × 10^4) layer electrode (ϕ = ca. 400 nm) on an ITO substrate (a) at 10 C rate and (b) in the range of 10−120 C rate. The electrolyte was a 0.1 M (n-C_4H_9)$_4$NClO$_4$/CH_3CN solution. Inset: cycle performance at 10 C rate for charging and discharging.

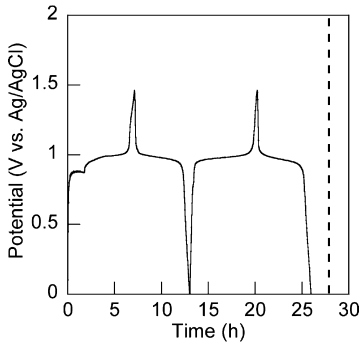

Figure 5. Charging/discharging curve of the 0.1 M PNB-*g*-PTMA (M_n = 2.2 × 10^5) solution in a half-cell of a flow cell system at 1 C rate, which referred to the capacity in a volume of the working unit (i.e., 1/7.5 C for the total capacity of the cell). The electrolyte was a 0.1 M (n-C_4H_9)$_4$NClO$_4$ in ethylene carbonate/diethyl carbonate (1/1 in v/v).

the Cottrell plots for the semi-infinite diffusion, which prevailed at the early stage of electrolysis (Figure S6), were comparable to those of other radical polymers.[25,60] These results indicates that counterions could swim throughout the bottlebrush architecture smoothly even near the backbone to support the quantitative redox reaction.

The charge-storage capability of PNB-*g*-PTMA as a redox-active nanomaterial was examined in a flow cell system based on the characteristics of bottlebrush polymers such as low viscosity and controllable dimension in a solution state, in contrast to the thin layer electrode of the aggregated PNB-*g*-PTMA. A half-cell (Figure S7) under the circulation of 0.1 M PNB-*g*-PTMA (M_n = 2.2 × 10^5) solution through a flow channel exhibited a plateau potential at 1.0 V vs Ag/AgCl in a charging/discharging test at 1 C rate, which referred to the capacity in a volume of the working unit (i.e., 1/7.5 C for the total capacity of the cell) (Figure 5). The charge capacity was 95% of the theoretical capacity, which agreed well with the quantitative capacity observed with the thin layer electrode. Less than 1% of the PNB-*g*-PTMA with a 41 nm of the number-average diameter permeated the porous separator with a 27 nm of the pore size from the flow channel to the counter unit after a circulation of the solution for 24 h. These results clearly demonstrated that the discrete molecular dimension of PNB-*g*-PTMA which was sufficiently larger than the pore size of the nanoporous separator was an essential factor for the charging/discharging cyclability in the flow cell system.

CONCLUSION

Radical-crowded bottlebrush polymers were successfully synthesized via a "grafting-through" approach with anionic polymerization and subsequent ring-opening metathesis polymerization using a norbornene-substituted diphenylhexyllithium and Grubbs catalysts, respectively. The sequence process consistently conducted direct polymerization of radical monomers. Structure analyses of the radical bottlebrush polymers by dynamic light scattering and atomic force microscopy measurements proved that the "grafting-through" approach gave us an easy access to the radical bottlebrush polymers with the well-defined sizes, which were tunable by both side chain and main chain lengths. The thin layer electrode of the radical bottlebrush polymer displayed the quantitative redox capacity at rapid charging/discharging as well as other radical polymers despite that the redox-active center, TEMPO, densely located in the closely packed macromolecular side chains. The quantitative charging/discharging of the radical bottlebrush polymer solution in the flow cell system indicated that shape-controlled redox-active polymers could be new candidates for electrode-active materials in redox flow batteries. The radical bottlebrush polymer combines the excellent electrochemical properties unique to the radical polymer and potentially size-tunable macromolecular architectures between nano- and microscale, which promise to expand potential applications of redox-active nanomaterials.

ASSOCIATED CONTENT

Supporting Information

Experimental section with synthetic procedures, additional figures, and characterizations. This material is available free of charge via the Internet at http://pubs.acs.org.

AUTHOR INFORMATION

Corresponding Authors

*E-mail oyaizu@waseda.jp (K.O.).
*E-mail nishide@waseda.jp (H.N.).

Notes

The authors declare no competing financial interest.

■ ACKNOWLEDGMENTS

This work was partially supported by Grants-in-Aid for Scientific Research (Nos. 25288056, 26620108, 25107733, and 24225003) from MEXT, Japan. We thank Dr. Shigeyuki Iwasa and Dr. Kentaro Nakahara of NEC Co. for technical discussion on the TEMPO-containing polymer synthesis. Support by the research project "Functional Redox Polymers" from Waseda Research Institute for Science and Engineering is also acknowledged.

■ REFERENCES

(1) Nishide, H.; Oyaizu, K. In *Encyclopedia of Sustainability Science and Technology*; Meyers, R. A., Ed.; Springer: New York, 2012; pp 235−246.
(2) Nishide, H.; Oyaizu, K. *Science* **2008**, *319*, 737−738.
(3) Oyaizu, K.; Nishide, H. *Adv. Mater.* **2009**, *21*, 2339−2344.
(4) Sen, S.; Saraidaridis, J.; Kim, S. Y.; Palmore, G. T. R. *ACS Appl. Mater. Interfaces* **2013**, *5*, 7825−7830.
(5) Chen, H. Y.; Armand, M.; Courty, M.; Jiang, M.; Grey, C. P.; Dolhem, F.; Tarascon, J. M.; Poizot, P. *J. Am. Chem. Soc.* **2009**, *131*, 8984−8988.
(6) Xu, W.; Read, A.; Koech, P. K.; Hu, D. H.; Wang, C. M.; Xiao, J.; Padmaperuma, A. B.; Graff, G. L.; Liu, J.; Zhang, J. G. *J. Mater. Chem.* **2012**, *22*, 4032−4039.
(7) Pirnat, K.; Dominko, R.; Cerc-Korosec, R.; Mali, G.; Genorio, B.; Gaberscek, M. *J. Power Sources* **2012**, *199*, 308−314.
(8) Shimizu, A.; Kuramoto, H.; Tsujii, Y.; Nokami, T.; Inatomi, Y.; Hojo, N.; Suzuki, H.; Yoshida, J. *J. Power Sources* **2014**, *260*, 211−217.
(9) Hanyu, Y.; Ganbe, Y.; Honma, I. *J. Power Sources* **2013**, *221*, 186−190.
(10) Renault, S.; Geng, J. Q.; Dolhem, F.; Poizot, P. *Chem. Commun.* **2011**, *47*, 2414−2416.
(11) Geng, J. Q.; Bonnet, J. P.; Renault, S.; Dolhem, F.; Poizot, P. *Energy Environ. Sci.* **2010**, *3*, 1929−1933.
(12) Renault, S.; Gottis, S.; Barres, A. L.; Courty, M.; Chauvet, O.; Dolhem, F.; Poizot, P. *Energy Environ. Sci.* **2013**, *6*, 2124−2133.
(13) Armand, M.; Grugeon, S.; Vezin, H.; Laruelle, S.; Ribiere, P.; Poizot, P.; Tarascon, J. M. *Nat. Mater.* **2009**, *8*, 120−125.
(14) Walker, W.; Grugeon, S.; Mentre, O.; Laruelle, S. p.; Tarascon, J.-M.; Wudl, F. *J. Am. Chem. Soc.* **2010**, *132*, 6517−6523.
(15) Liang, Y. L.; Zhang, P.; Chen, J. *Chem. Sci.* **2013**, *4*, 1330−1337.
(16) Matsunaga, T.; Kubota, T.; Sugimoto, T.; Satoh, M. *Chem. Lett.* **2011**, *40*, 750−752.
(17) Liang, Y. L.; Zhang, P.; Yang, S. Q.; Tao, Z. L.; Chen, J. *Adv. Energy Mater.* **2013**, *3*, 600−605.
(18) Morita, Y.; Nishida, S.; Murata, T.; Moriguchi, M.; Ueda, A.; Satoh, M.; Arifuku, K.; Sato, K.; Takui, T. *Nat. Mater.* **2011**, *10*, 947−951.
(19) Sultana, I.; Rahman, M. M.; Wang, J. Z.; Wang, C. Y.; Wallace, G. G.; Liu, H. K. *Solid State Ionics* **2012**, *215*, 29−35.
(20) Nakahara, K.; Oyaizu, K.; Nishide, H. *Chem. Lett.* **2011**, *40*, 222−227.
(21) Oyaizu, K.; Nishide, H. In *Encyclopedia of Radicals in Chemistry, Biology and Materials*; Chatgilialoglu, C., Studer, A., Eds.; Wiley: Chichester, 2012.
(22) Song, Z. P.; Zhou, H. S. *Energy Environ. Sci.* **2013**, *6*, 2280−2301.
(23) Oyaizu, K.; Nishide, H. In *Advanced Nanomaterials*, Geckeler, K., Nishide, H., Eds.; Wiley-VCH: Weinheim, 2010; pp 319−332.
(24) Huskinson, B.; Marshak, M. P.; Suh, C.; Er, S.; Gerhardt, M. R.; Galvin, C. J.; Chen, X. D.; Aspuru-Guzik, A.; Gordon, R. G.; Aziz, M. J. *Nature* **2014**, *505*, 195−198.
(25) Oyaizu, K.; Ando, Y.; Konishi, H.; Nishide, H. *J. Am. Chem. Soc.* **2008**, *130*, 14459−14461.
(26) Oyaizu, K.; Suga, T.; Yoshimura, K.; Nishide, H. *Macromolecules* **2008**, *41*, 6646−6652.
(27) Yoshihara, S.; Isozumi, H.; Kasai, M.; Yonehara, H.; Ando, Y.; Oyaizu, K.; Nishide, H. *J. Phys. Chem. B* **2010**, *114*, 8335−8340.
(28) Hyakutake, T.; Park, J.-Y.; Yonekuta, Y.; Oyaizu, K.; Nishide, H.; Advincula, R. *J. Mater. Chem.* **2010**, *20*, 9616−9618.
(29) Suga, T.; Pu, Y.-J.; Oyaizu, K.; Nishide, H. *Bull. Chem. Soc. Jpn.* **2004**, *77*, 2203−2204.
(30) Yonekuta, Y.; Oyaizu, K.; Nishide, H. *Chem. Lett.* **2007**, *36*, 866−867.
(31) Choi, W.; Ohtani, S.; Oyaizu, K.; Nishide, H.; Geckeler, K. E. *Adv. Mater.* **2011**, *23*, 4440−4443.
(32) Nakahara, K.; Oyaizu, K.; Nishide, H. *J. Mater. Chem.* **2012**, *22*, 13669−13673.
(33) Janoschka, T.; Hager, M. D.; Schubert, U. S. *Adv. Mater.* **2012**, *24*, 6397−6409.
(34) Kim, J.-K.; Scheers, J.; Ahn, J.-H.; Johansson, P.; Matic, A.; Jacobsson, P. *J. Mater. Chem. A* **2013**, *1*, 2426−2430.
(35) Vasilyeva, S. V.; Unur, E.; Walczak, R. M.; Donoghue, E. P.; Rinzler, A. G.; Reynolds, J. R. *ACS Appl. Mater. Interfaces* **2009**, *1*, 2288−2297.
(36) Koshika, K.; Sano, N.; Oyaizu, K.; Nishide, H. *Chem. Commun.* **2009**, 836−838.
(37) Suga, T.; Ohshiro, H.; Sugita, S.; Oyaizu, K.; Nishide, H. *Adv. Mater.* **2009**, *21*, 1627−1630.
(38) Koshika, K.; Sano, N.; Oyaizu, K.; Nishide, H. *Macromol. Chem. Phys.* **2009**, *210*, 1989−1995.
(39) Zhuang, X.; Zhang, H.; Chikushi, N.; Zhao, C.; Oyaizu, K.; Chen, X.; Nishide, H. *Macromol. Biosci.* **2010**, *10*, 1203−1209.
(40) Koshika, K.; Chikushi, N.; Sano, N.; Oyaizu, K.; Nishide, H. *Green. Chem.* **2010**, *12*, 1573−1575.
(41) Zhuang, X.; Xiao, C.; Oyaizu, K.; Chikushi, N.; Chen, X.; Nishide, H. *J. Polym. Sci., Part A* **2010**, *48*, 5404−5410.
(42) Oyaizu, K.; Sukegawa, T.; Nishide, H. *Chem. Lett.* **2011**, *40*, 184−185.
(43) Suga, T.; Sugita, S.; Ohshiro, H.; Oyaizu, K.; Nishide, H. *Adv. Mater.* **2011**, *23*, 751−754.
(44) Yoshihara, S.; Katsuta, H.; Isozumi, H.; Kasai, M.; Oyaizu, K.; Nishide, H. *J. Power Sources* **2011**, *196*, 7806−7811.
(45) Chikushi, N.; Yamada, H.; Oyaizu, K.; Nishide, H. *Sci. Chin. Chem.* **2012**, *55*, 822−829.
(46) Oyaizu, K.; Nishide, H. *Macromol. Symp.* **2012**, *317−318*, 248−258.
(47) Chae, I. S.; Koyano, M.; Sukegawa, T.; Oyaizu, K.; Nishide, H. *J. Mater. Chem. A* **2013**, *1*, 9608−9611.
(48) Kato, F.; Kikuchi, A.; Okuyama, T.; Oyaizu, K.; Nishide, H. *Angew. Chem., Int. Ed.* **2012**, *51*, 10177−10180.
(49) Sano, N.; Tomita, W.; Hara, S.; Min, C.-M.; Lee, J.-S.; Oyaizu, K.; Nishide, H. *ACS Appl. Mater. Interfaces* **2013**, *5*, 1355−1361.
(50) Kato, F.; Hayashi, N.; Murakami, T.; Okumura, C.; Oyaizu, K.; Nishide, H. *Chem. Lett.* **2010**, *39*, 464−465.
(51) Oyaizu, K.; Hayo, N.; Sasada, Y.; Kato, F.; Nishide, H. *Dalton Trans.* **2013**, *42*, 16090−16095.
(52) Kato, R.; Kato, F.; Oyaizu, K.; Nishide, H. *Chem. Lett.* **2014**, *43*, 480−482.
(53) Oyaizu, K.; Ikeda, H.; Hayo, N.; Kato, F.; Nishide, H. *Chem. Lett.* **2014**, *43*, 1134−1136.
(54) Yonekuta, Y.; Susuki, K.; Oyaizu, K.; Honda, K.; Nishide, H. *J. Am. Chem. Soc.* **2007**, *129*, 14128−14129.
(55) Suga, T.; Takeuchi, S.; Ozaki, T.; Sakata, M.; Oyaizu, K.; Nishide, H. *Chem. Lett.* **2009**, *38*, 1160−1161.
(56) Takahashi, Y.; Hayashi, N.; Oyaizu, K.; Honda, K.; Nishide, H. *Polym. J.* **2008**, *40*, 763−767.
(57) Amb, C. M.; Dyer, A. L.; Reynolds, J. R. *Chem. Mater.* **2011**, *23*, 397−415.
(58) Beaujuge, P. M.; Amb, C. M.; Reynolds, J. R. *Acc. Chem. Res.* **2010**, *43*, 1396−1407.
(59) Tokue, H.; Oyaizu, K.; Sukegawa, T.; Nishide, H. *ACS Appl. Mater. Interfaces* **2014**, *6*, 4043−4049.

(60) Oyaizu, K.; Kawamoto, T.; Suga, T.; Nishide, H. *Macromolecules* **2010**, *43*, 10382−10389.
(61) Nakahara, K.; Iriyama, J.; Iwasa, S.; Suguro, M.; Satoh, M.; Cairns, E. J. *J. Power Sources* **2007**, *165*, 870−873.
(62) Nesvadba, P.; Bugnon, L.; Pascal, M.; Novák, P. *Chem. Mater.* **2010**, *22*, 783−788.
(63) Chae, I. S.; Koyano, M.; Oyaizu, K.; Nishide, H. *J. Mater. Chem. A* **2013**, *1*, 1326−1333.
(64) Miyanishi, S.; Zhang, Y.; Hashimoto, K.; Tajima, K. *Macromolecules* **2012**, *45*, 6424−6437.
(65) Ku, S.-Y.; Brady, M. A.; Treat, N. D.; Cochran, J. E.; Robb, M. J.; Kramer, E. J.; Chabinyc, M. L.; Hawker, C. J. *J. Am. Chem. Soc.* **2012**, *134*, 16040−16046.
(66) Suga, T.; Takeuchi, S.; Nishide, H. *Adv. Mater.* **2011**, *23*, 5545−5549.
(67) Ibe, T.; Frings, R. B.; Lachowicz, A.; Kyo, S.; Nishide, H. *Chem. Commun.* **2010**, *46*, 3475−3477.
(68) Zhang, M.; Müller, A. H. E. *J. Polym. Sci., Part A: Polym. Chem.* **2005**, *43*, 3461−3481.
(69) Tsukahara, Y.; Tsutsumi, K.; Okamoto, Y. *Macromolecules* **1994**, *27*, 1662−1664.
(70) Müller, M.; Lunkenbein, T.; Schieder, M.; Gröschel, A. H.; Miyajima, N.; Förtsch, M.; Breu, J.; Caruso, F.; Müller, A. H. E. *Macromolecules* **2012**, *45*, 6981−6988.
(71) Huang, K.; Rzayev, J. *J. Am. Chem. Soc.* **2011**, *133*, 16726−16729.
(72) Runge, M. B.; Bowden, N. B. *J. Am. Chem. Soc.* **2007**, *129*, 10551−10560.
(73) Miyake, G. M.; Piunova, V. A.; Weitekamp, R. A.; Grubbs, R. H. *Angew. Chem., Int. Ed.* **2012**, *51*, 11246−11248.
(74) Sun, G.; Cho, S.; Clark, C.; Verkhoturov, S. V.; Eller, M. J.; Li, A.; Pavía-Jiménez, A.; Schweikert, E. A.; Thackeray, J. W.; Trefonas, P.; Wooley, K. L. *J. Am. Chem. Soc.* **2013**, *135*, 4203−4206.
(75) Rzayev, J. *ACS Macro Lett.* **2012**, *1*, 1146−1149.
(76) Schappacher, M.; Defieux, A. *Macromol. Chem. Phys.* **1997**, *3961*, 3953−3961.
(77) Deffieux, A.; Schappacher, M. *Macromolecules* **1999**, *32*, 1797−1802.
(78) Schappacher, M.; Deffieux, A. *Science* **2008**, *319*, 1512−1515.
(79) Ryu, S. W.; Hirao, A. *Macromolecules* **2000**, *33*, 4765−4771.
(80) Ryu, S. W.; Hirao, A. *Macromol. Chem. Phys.* **2001**, 1727−1736.
(81) Xia, Y.; Kornfield, J. A.; Grubbs, R. H. *Macromolecules* **2009**, *42*, 3761−3766.
(82) Gao, H.; Matyjaszewski, K. *J. Am. Chem. Soc.* **2007**, *129*, 6633−6639.
(83) Lee, H.; Jakubowski, W.; Matyjaszewski, K.; Yu, S.; Sheiko, S. S. *Macromolecules* **2006**, *39*, 4983−4989.
(84) Rzayev, J. *Macromolecules* **2009**, *42*, 2135−2141.
(85) Huang, K.; Canterbury, D. P.; Rzayev, J. *Chem. Commun.* **2010**, *46*, 6326−6328.
(86) Li, Z.; Ma, J.; Cheng, C.; Zhang, K.; Wooley, K. L. *Macromolecules* **2010**, *43*, 1182−1184.
(87) Cheng, C.; Qi, K.; Khoshdel, E.; Wooley, K. L. *J. Am. Chem. Soc.* **2006**, *128*, 6808−6809.
(88) Hawker, C. J.; Bosman, A. W.; Harth, E. *Chem. Rev.* **2001**, *101*, 3661−3688.
(89) Nishide, H.; Iwasa, S.; Pu, Y.-J.; Suga, T.; Nakahara, K.; Satoh, M. *Electrochim. Acta* **2004**, *50*, 827−831.
(90) Suga, T.; Konishi, H.; Nishide, H. *Chem. Commun.* **2007**, 1730−1732.
(91) Choi, W.; Endo, S.; Oyaizu, K.; Nishide, H.; Geckeler, K. E. *J. Mater. Chem. A* **2013**, *1*, 2999−3003.
(92) Sukegawa, T.; Kai, A.; Oyaizu, K.; Nishide, H. *Macromolecules* **2013**, *46*, 1361−1367.
(93) Sukegawa, T.; Omata, H.; Masuko, I.; Oyaizu, K.; Nishide, H. *ACS Macro Lett.* **2014**, *3*, 240−243.
(94) Reutenauer, S.; Hurtrez, G.; Dumas, P. *Macromolecules* **2001**, *37*, 755−760.
(95) Gerle, M.; Fischer, K.; Roos, S.; Mu, A. H. E.; Schmidt, M.; Sheiko, S. S.; Prokhorova, S.; Mo, M. *Macromolecules* **1999**, *32*, 2629−2637.